

pubs.acs.org/JPCC Article

Interplay between Energy and Charge Transfers in a Polyaromatic Triplet Donor-Acceptor Dyad

Young Ju Yun, Nareshbabu Kamatham, Manoj K. Manna, Jingbai Li, Shuyang Liu, Gary P. Wiederrecht, David J. Gosztola, Benjamin T. Diroll, Andrey Yu Rogachev, and A. Jean-Luc Ayitou*



Cite This: https://dx.doi.org/10.1021/acs.jpcc.0c01530



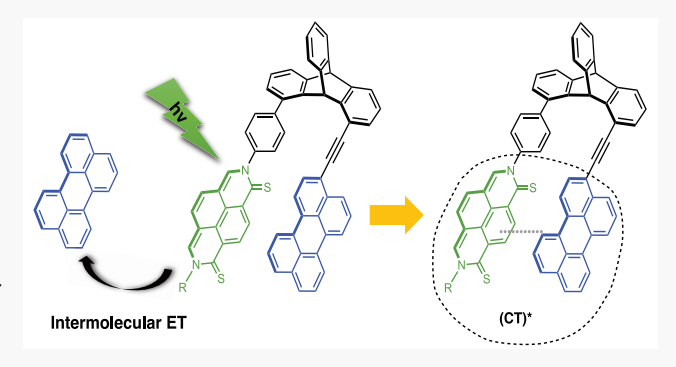
ACCESS

III Metrics & More

Article Recommendations

s Supporting Information

ABSTRACT: We report the synthesis and photophysical characterization of a triplet donor—acceptor dyad (3), which was constructed from a quinoidal naphthalene thioamide triplet sensitizer 1 and a perylene derivative 2 as the acceptor. The dyad of interest exhibits convoluted photophysical characteristics from the donor and acceptor chromophores. The kinetic analysis of the phosphorescence of 3 produced two lifetimes τ_1 = 1.1 ms and τ_2 = 20 ms. The shorter component was attributed to the phosphorescence lifetime of the sensitizer $^3(1)^*$ moiety (within the dyad) and the longer lifetime can be assigned to either the triplet state of the acceptor $^3(2)^*$ or a charge transfer (CT)* species. This result was further corroborated with time-resolved transient absorption studies which revealed the CT band in the transient spectrum of



the dyad. In this picture, the $1\cdots 2$ interactions, which led to the formation of the CT species, was found to be the dominant photodynamics. Alternatively, dyad 3 was used to sensitize free perylene acceptor; the bimolecular $^3(3)^* \rightarrow$ perylene triplet energy transfer allowed triplet—triplet annihilation based photon upconversion to generate anti-Stokes photoluminescence of perylene using a 532 nm excitation source.

■ INTRODUCTION

Donor-acceptor chromophoric systems (D-A) are important scaffolds for several light-harvesting/initiated processes 1,2 and devices including light emitting diodes, 3-6 photocatalytic/ redox systems, ^{7,8} and photovoltaics cells. ⁹⁻¹² In a **D-A** system, the donor moiety often plays the role of the antenna that is well positioned to maximize ideal dipole-dipole or orbitals interactions with the acceptor moiety upon photoexcitation in such a way to allow efficient $D \to A$ energy or charge transfer (ET and CT, respectively). 13-15 In recent years, the development of D-A systems has mainly relied on polyaromatic acceptors and cyanine dyes 16,17 or other coordination complex¹⁸ donors which are employed as the antenna. Unquestionably, these donor chromophores exhibit attractive photophysics which can be tailored for many of the aforementioned applications. However, from a synthetic point of view, the assembling of D-A systems from structurally incompatible components, coordination complexes and purely organic scaffolds, especially when the acceptor unit also exhibit complex structural features may seem challenging.

Purely organic **D**-**A** systems can be prepared easily and handled under ambient conditions. These systems could also be further tailored for organic optoelectronic devices. ^{14,19–23} In purely organic **D**-**A** systems, the donor and acceptor chromophores can be tethered onto a rigid template that

would be conducive to maximum intradyad dipole—dipole or orbital interactions. This synthetic strategy has been pioneered by Wasielewski et al., who showcased rigid template-based polyaromatic chromophoric dyads to investigate ET and CT as well as singlet fission in π -stacked/conjugated chromophoric systems. ^{13,24–26} In the present study, we devised a triptycene-based **D**–**A** dyad 3 that is constructed from a quinoidal naphthyl thioamide triplet sensitizer QDN 1 and a perylene-based acceptor Per 2 (Figure 1). Our design is inspired by the structural and photophysical compatibilities of the donor and acceptor chromophores, which we used in previous triplet sensitization and triplet—triplet annihilation based photon upconversion (TTA-UC) studies. ^{27,28}

Herein, we report the synthesis and photophysical characterization of a triptycene-based dyad 3, which features the triplet sensitizer (triplet energy donor) QDN 1 and the energy acceptor Per 2 (Figure 1). This work aims at unravelling the ground and excited state optoelectronic coupling of 1 and 2,

Received: February 21, 2020 Revised: May 19, 2020 Published: May 19, 2020



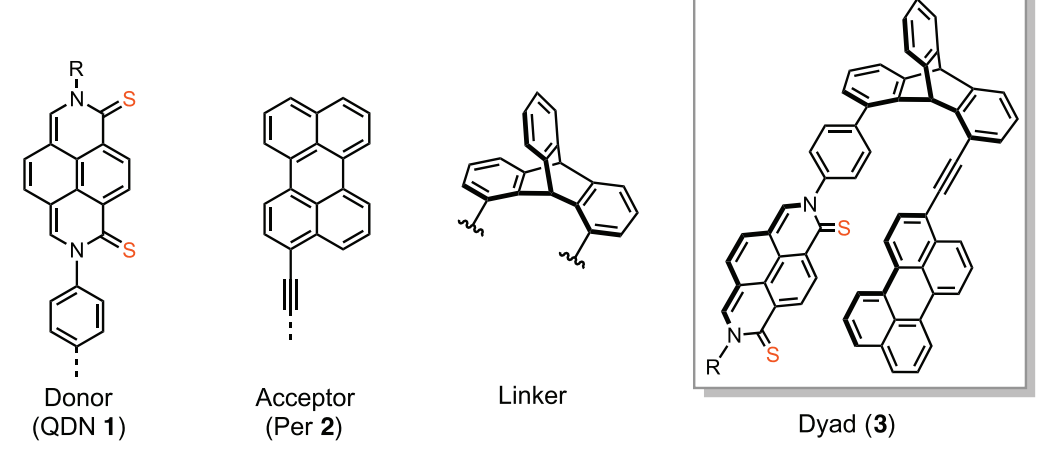


Figure 1. Chemical structures of triplet energy donor QDN 1, triplet energy acceptor Per 2, linker, and QDN-Per dyad 3. $R = n - C_8 H_{17}$.

Scheme 1. Synthesis of Triptycene-Based Donor-Acceptor Dyad 3^a

^aThe synthetic procedures of precursors/starting reagents are presented in the Supporting Information, Schemes S2–10.

which can interact through-space only in the slip-stack conformation within the dyad. Using a combination of pump—probe spectroscopy techniques and computational tools, we established that, upon photoexcitation, the donor—acceptor interactions in dyad 3 produces charge transfer states (CT)*, which are manifested by the apparent suppression of the expected intradyad $\mathbf{D} \to \mathbf{A}$ triplet energy flow.

METHODS

Experimental Section. The synthetic procedures for all precursors of dyad 3 are extensively described in the Supporting Information (Scheme S1). All NMR characterizations were carried out on a Bruker 300 MHz spectrometer at 298 K. High-resolution mass spectrum data were recorded on a Bruker microTOF II or Shimadzu IT-TOF spectrometers in positive (ESI+) ion mode. All spectroscopy measurements were performed using spectroscopy-grade solvents. UV—vis absorption spectra were recorded on an Ocean Optics spectrometer (DH-MINI UV—vis—NIR light source and QE-Pro detector). Emission spectra were recorded on an Edinburgh Instrument FLS980 spectrometer. Time-resolved pump—probe spectroscopy was performed using an amplified

Ti:sapphire laser system (Spectra Physics Spitfire) equipped with an optical parametric amplifier (OPA, Light Conversion, TOPAS). This system produces 130 fs pulses at 5 kHz centered at 800 nm. 95% of the output from the amplifier is directed to the OPA to generate tunable pump pulses in the visible and near-infrared spectral regions. For operation with 130 fs temporal resolution, the pump pulse and the remaining 5% of output from the amplifier are directed to a transient absorption spectrometer (Helios from Ultrafast Systems), where the 5% output is used to generate a continuum probe pulse extending from 450 nm to 1400 nm by focusing into a thin sapphire window. The pump pulse is chopped at half the repetition rate to measure a difference spectrum for the transient absorption measurement. The incident pump pulse for these experiments at 470 or 520 nm had energy on the sample of 400 nJ per pulse, focused to a 200- μ m-diameter spot. The transmitted probe light was collected and fiber optically coupled to a spectrograph that used a visible (Si) array detector. Data were collected for continuum wavelengths from 450 to 750 nm as a function of delay track position for the continuum probe relative to the undelayed pump pulse. The temporal chirp of the data was experimentally determined and corrected before analysis. For longer time scale processes, the probe light comes from a continuum light source (EOS from Ultrafast Systems). In this case, the system operates at 1 kHz and has a time resolution of 200 ps/point. Decay times of several hundred microseconds can be measured. Upconverted emission measurements were performed by focusing a continuous wave 532 nm laser to ${\sim}60~\mu{\rm m}$ beam diameter on to cuvettes of sample. Emitted light was collected and focused into a fiber and routed through a monochromator to a CCD. A band-stop filter was used to block excitation light.

Calculation Details. Geometry optimizations were performed using a highly efficient electronic structure approach, PBEh-3c,²⁹ where a hybrid Perdew-Burke-Ernzerhof (PBE) functional with 42% of nonlocal Fock-exchange is employed with a double- ζ quality Gaussian-type atomic orbital basis set, def2-mSVP. The basis set superposition errors (BSSE) and London dispersion effects were accounted by the implementation of geometrical counterpart (gCP)30 and dispersion correction (D3)^{31,32} schemes, respectively. In order to speed up calculations, the "resolution-of-identity" (RI)33 approximation RIJCOSX (RI-J for Coulomb integrals and COSX numerical integration for HF exchange) and the auxiliary def2/J basis set.34 The optimized geometries were then used in single-point calculations at PBEO/cc-pVTZ level of theory to provide insight into details of electronic structure of target compounds and to compute the excitation energies with help of the time-dependent density functional theory (TD-DFT). The solution effect of dichloromethane (DCM) was included by conduct-like polarizable continuum model (CPCM). All calculations were performed using ORCA 4.0.0 suite of program.3

Synthesis of Dyad 3. Dyad 3 was synthesized following a convergent synthetic method as depicted in Scheme 1. The synthetic strategy used for QDN 1 was previously reported from our group. ³⁶ Per 2 and QDN 1 were used in sequential Sonogashira and Suzuki—Miyaura coupling reactions to afford the final dyad 3 in 20% isolated yield after purification by flash column chromatography.

Triptycene-Per (Trip-2) (30 mg, 1.0 equiv., 0.05 mmol), Pd(PPh₃)₄ (1.6 mg, 3 mol %), and QDN 1 (29.4 mg, 1.2 equiv., 0.05 mmol) were added to a 10 mL solution of 1,4dioxane. Then, an aqueous solution of K₂CO₃ (12.6 mg, 2.0 equiv., 0.01 mmol) in 2 mL of water was added to the reaction flask. The new mixture was purged with a stream of Ar. Next, the solution was heated at 140 \pm 5 °C for 72 h under constant stirring. After, the resulting solution was cooled to room temperature, and the expected compound was guenched with 20 mL of water. The expected compound was extracted with 20% acetone/80% dichloromethane solvent system. The combined organic fraction was concentrated in vacuo under reduced pressure and the purified by flash column chromatography on silica gel using dichloromethane as the eluent. The expected dyad 3 was obtained as a dark-wine colored solid. Yield: 9 mg, 20%.

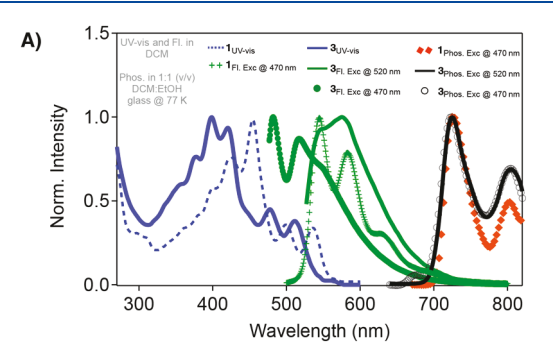
¹H NMR (300 MHz, CD_2Cl_2) δ 9.09–8.99 (m, 3H), 8.51–8.42 (m, 3H), 7.80–7.58 (m, 14H), 7.47–7.36 (m, 8H), 7.04–6.88 (m, 5H), 4.81–4.76 (t, J = 15 Hz, 2H), 2.03–1.98 (t, J = 15 Hz, 2H), 1.46–1.32 (m, 10H), 0.91 (m, 3H).

 13 C NMR (75 MHz, CD₂Cl₂) δ 178.8, 178.7, 160.1, 160.0, 148.1, 145.3, 145.2, 145.1, 140.2, 140.1, 135.1, 134.8, 134.7, 134.1, 133.0, 132.9, 132.8, 132.5, 132.5, 132.1, 131.2, 131.1, 131.0, 130.7, 130.6, 130.5, 130.5, 130.3, 130.2, 130.1, 130.0, 129.4, 129.3, 128.9, 128.8, 128.6, 128.3, 127.3, 127.2, 126.6,

126.0, 125.8, 125.6, 125.2, 123.7, 123.3, 122.8, 122.3, 121.1, 120.8, 118.6, 118.5, 114.4, 114.3, 91.4, 85.1, 58.4, 31.8, 29.2, 29.2, 28.1, 26.8, 26.7, 22.6, 13.8.

■ RESULTS AND DISCUSSION

UV-vis and Emission Spectroscopy. Figure 2A shows the convoluted UV-vis transitions of QDN 1 and Per 2



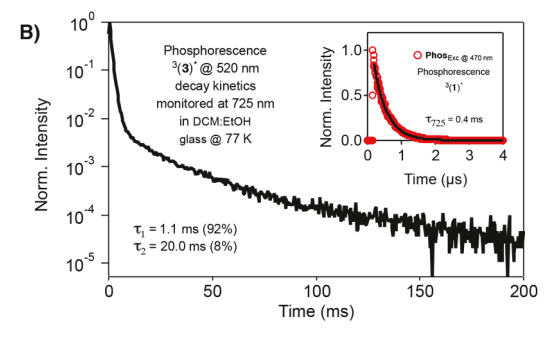


Figure 2. (A) UV—vis and emission profiles of QDN 1 and dyad 3; (B) phosphorescence decay trace (monitored at 725 nm) of dyad 3 at 77 K upon 520 nm excitation. Inset: Phosphorescence decay trace (monitored at 725 nm) of QDN 1 at 77 K upon 520 nm excitation.

(Supporting Information, Figures S22 and S23) into the absorption profile of dyad 3 between 300 and 600 nm with a $\lambda_{\rm max}$ at 398 nm and a minor band at 450–470 nm, which might be ascribed to a ground state charge transfer derivative of 3. Nevertheless, we believe that the ground state intradyad 1...2 through-space interaction seems less pronounced than the excited state dynamics of the dyad once the QDN antenna is photoexcited. It is important to note that perylene does not absorb beyond 450 nm, but the tail of the UV-vis profile of Per 2 does reach 470 nm (Supporting Information, Figure S22). Thus, if dyad 3 was excited at wavelength 450-470 nm, one should expect to see emission bands that would resemble the emission spectra that are characteristic of the isolated QDN 1 and Per 2 (Figure 2A and Supporting Information, Figures S20, S21, and S23). As shown in Figure 2A, the recorded emission band of dyad 3 with excitation at 470 nm seemingly resembles the convoluted fluorescence emissions from QDN 1 and Per 2 (Figure 2A and Supporting Information, Figure S22) suggesting no effective coupling between the two chromophoric units. Nevertheless, when dyad 3 was excited at 520 nm, the recorded fluorescence band is broadened and uncharacteristic of the emissions from isolated QDN 1. From these results, we hypothesized that the fluorescence emissions of 3 is likely the mixed transitions from the lowest singlet excited state of QDN 1 and a charge transfer state (CT)*, since the electronic bandgap of QDN 1

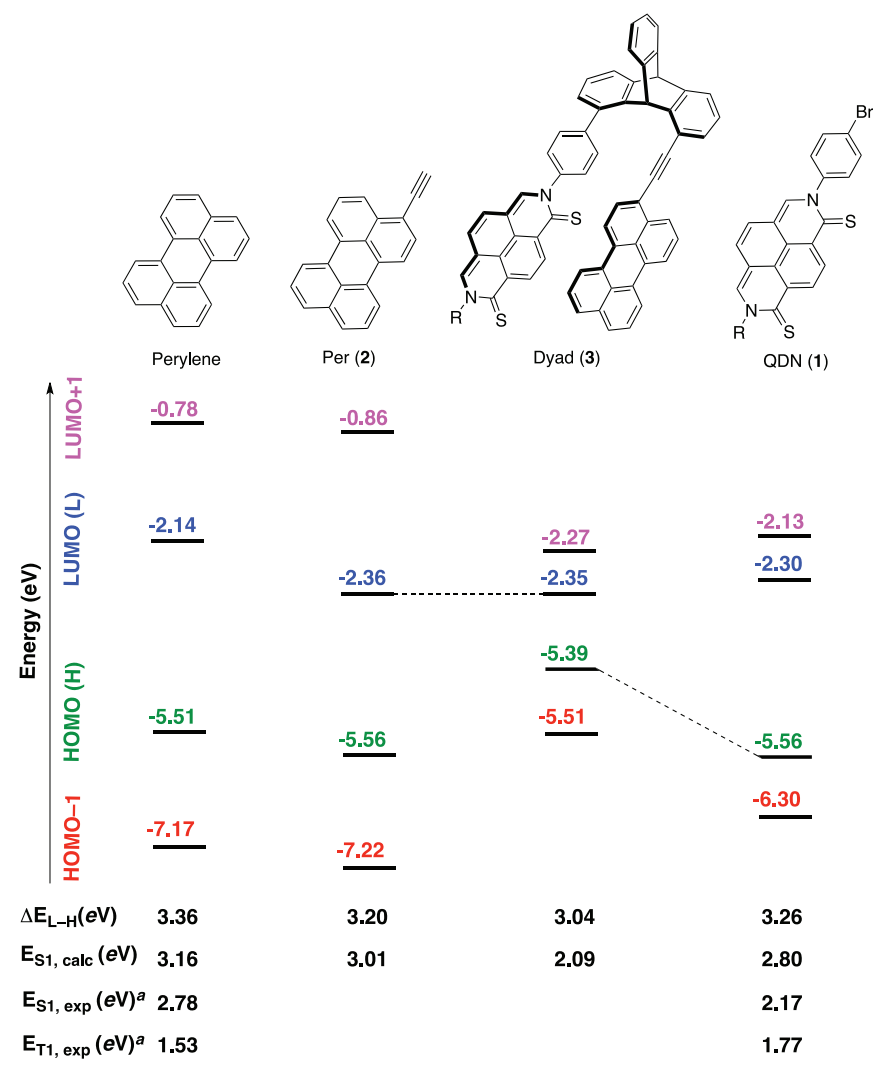


Figure 3. Optoelectronic bandgap of QDN 1, perylene, Per 2, and dyad 3. Calculations were performed (for R = CH₃) at PBE0/cc-pVTZ level of theory with solvent dichloromethane (see the Supporting Information for details). $\Delta E_{\rm L-H} = E_{\rm LUMO} - E_{\rm HOMO}$; $E_{\rm S1, calc}$ = computed excitation energy of S₁ state; $E_{\rm S1, exp}$ and $E_{\rm T1, exp}$ = energy levels of the lowest singlet and triplet excited state. ^aThe $E_{\rm S1, exp}$ and $E_{\rm T1, exp}$ values for 1 were estimated from the absorption and emission spectra ($\Phi_{\rm FI} = 0.2\%$ and $\Phi_{\rm ISC} = 98\%$); the $E_{\rm S1, exp}$ and $E_{\rm T1, exp}$ values for perylene were taken from ref 27.

and Per 2 can facilitate CT interaction as depicted in Figure 3. In this picture, it is likely that the photoinduced Dexter-type ET channel would be less pronounced in the dyad, whereas bimolecular $(1)^*$ or $(3)^* \rightarrow$ perylene ET can still occur as revealed in Figure 3 and in our previous study.27 Charge transfer in 3 has been revealed by time-dependent density functional theory (TD-DFT) calculations, where the predicted S_1 shows HOMO \rightarrow LUMO transition from 1 to Per 2. The computed S₁ is 2.09 eV lower than 1 (cal. 2.80 eV) and has a weak oscillator strength (0.02). It suggests that the small absorption of 3 near 550 nm (not observed in 1) could rise from the charge transfer in S₁. It is easier to see (from the orbitals energies calculations) that the intradyad (1)*...2 interactions would facilitate relaxation of the excited dyad (3)* to a lower state presumably the ${}^{1}(CT)^{*}$ or ${}^{3}(CT)^{*}$ states. Similar observations were formerly documented in π -stacked donor-acceptor supramolecular chromophores. 37,38

Furthermore, we hypothesize that the (CT)* species can also populate the dyad triplet state, but that process could be reversible. Photoexcitation (at 470 and 520 nm) of dyad 3 in a glassy matrix at 77 K produced a phosphorescence band that is similar to the emission characteristics of the parent QDN 1

(Supporting Information, Figures S19–21 and S23 and Figure 2B) indicating that the intradyad $^3(1)^* \rightarrow 2$ triplet energy flow is less efficient due to unmatched optoelectronic bandgap of 1 and 2. While the phosphorescence decay kinetic of the isolated QDN 1 was fit with a monoexponential function to produce a lifetime of $\tau_{725} = 0.4$ ms, the kinetic of dyad 3 phosphorescence produced a decay trace with two lifetimes $\tau_1 = 1.1$ ms (92%) and $\tau_2 = 20$ ms (8%; Figure 2B). Presumably, the short lifetime (major component) is the actual phosphorescence lifetime from the QDN $^3(1)^*$ moiety (within the dyad) and the long lifetime might originate from either Per $^3(2)^*$ or the triplet charge transfer state $^3(CT)^*$.

Transient Absorption Spectroscopy. Next, we used pump–probe spectroscopy (TA) method to unravel the dynamics of the excited state of dyad 3 (Figure 4). As shown in Figure 4B, upon laser excitation ($\lambda_{\rm Exc} = 520$ nm to avoid exciting the Per moiety), dyad 3 quickly populated the $S_{\rm 1or2}$ electronic states³⁶ followed by absorption of the singlet transient $^{1}(3)^{*}$ which exhibits similar characteristics (with ($\lambda_{\rm Abs} \approx 490$ nm) as the ones seen in the femtosecond-TA (fs-TA) of parent QDN 1 (Figure 4A)). However, the presence of a new band between 620 and 720 nm (for the dyad) is most

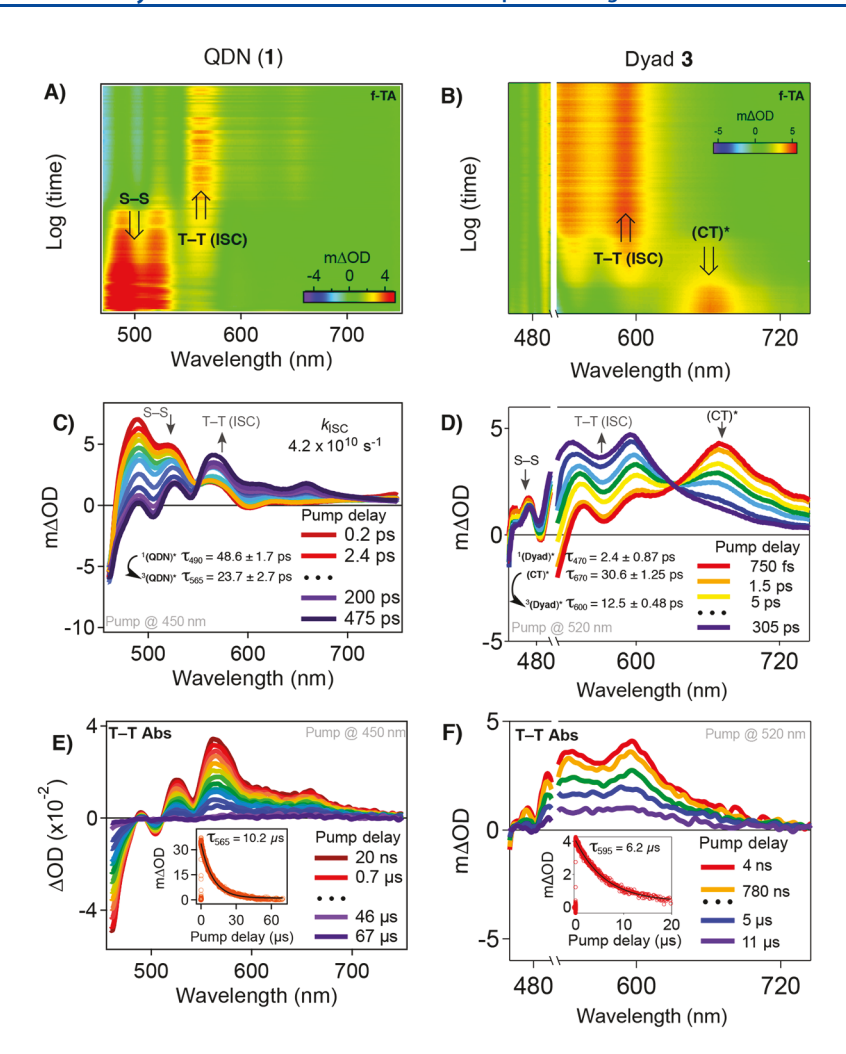


Figure 4. Femtosecond time-resolved transient absorption 2D intensity map of 1 (A) and 3 (B) and corresponding kinetics (C) for 1 and (D) for 3 recorded in oxygen-free THF with a sample of optical density: OD = 0.5 at λ_{Exc} = 450 nm (for 1) and λ_{Exc} = 520 nm (for 3), 0.4 μ J/pulse and 2 kHz repetition rate. (E and F) Nanosecond time-resolved transient absorption spectra and corresponding kinetics for 1 and 3 (respectively) in oxygen-free THF with a sample of optical density: OD = 0.5 at λ_{Exc} = 450 nm (for 1) and λ_{Exc} = 520 nm (for 3), 1 μ J/pulse and 1 kHz repetition rate.

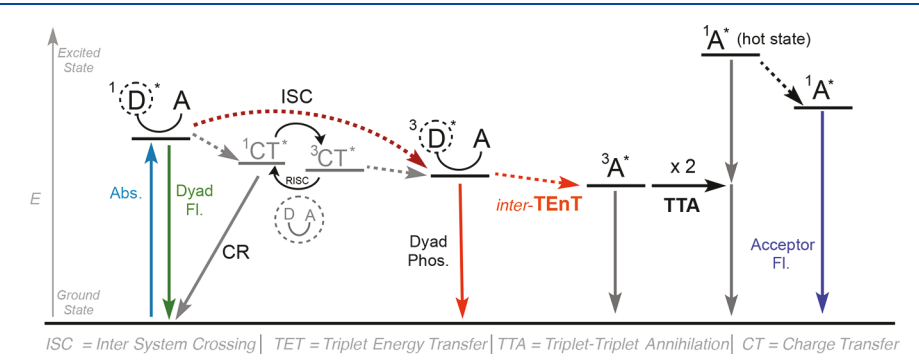


Figure 5. Photophysical pathway of dyad 3 (D-A). Also shown is the TTA-UC process in the presence of free acceptor perylene (A). Note: The energy levels of the CT states were positioned hypothetically with respect to the lowest excited states.

likely due to absorption of the CT transients. The isosbestic points at ca. 550 nm for 1 and 630 nm for 3 is indicative of ISC leading to the formation of the corresponding triplet transients (Figures 4C,D). The kinetics of the singlet transient of QDN 1 was evaluated with a monoexponential function producing a time constant of $\tau_{490} = 48.6$ ps, whereas the fs-TA of dyad 3 showed additional band centered at 630 nm besides the actual

singlet transient absorption at 490 nm (Figure 4B). The band at 490 nm was fitted with a monoexponential function with time constants $\tau=2.4$ ps and the one at 630 nm gave a time constant of $\tau=30.6$ ps. We assigned the transient band at 630 nm to the (CT)* transient/species. Furthermore, in the fs-TA of the dyad, the presence of a new band at ca. 545 nm in addition to the triplet transient band from the QDN moiety

(Figure 4B) is suggestive of either the ³(CT)* transient or the triplet transient from the Per moiety (Figures 4B,D).

Expectedly, the long-lived features in the fs-TA of dyad 3 were also revealed in the triplet transient spectrum (Figure 4F). Time resolved nanosecond-TA (ns-TA) triplet—triplet absorption of 3 showed a much weaker spectrum in intensity which is 1 order of magnitude lower than the triplet absorption spectrum of parent QDN 1 (Figure 4E). We hypothesize that the plausible cause of the low triplet absorption intensity in the case of dyad 3 is likely a delocalization of the triplet state (from the QDN moiety) onto the Per moiety. The summary of the photophysical pathway of dyad 3 is summarized in Figure 5.

Application with Triplet-Triplet Annihilation Photon **Up-Conversion.** Since dyad 3 exhibits similar phosphorescence characteristics as the parent QDN 1 (Figure 2A), we attempted to use it as a light-harvesting triplet sensitizer to perform bimolecular triplet energy transfer to free perylene in solution.²⁷ This experiment will also shed light on the dynamics of intradyad vs intermolecular triplet energy flow with respect to the position of the optoelectronic states of the individual chromophores (1, perylene, and 2) as depicted in Figure 3. We showed earlier that intradyad Dexter-type ³(1)* → 2 energy flow would be hampered by the formation of the (CT)* species; on the other hand, one should expect ${}^{3}(3)^{*} \rightarrow$ perylene triplet energy transfer due to the compatibility of 1 or 3 with free perylene in term of optoelectronic bandgap. Upon excitation of an oxygen-free THF solution of dyad 3 and free perylene using a 532 nm diode laser, the delayed photoluminescence of perylene (420-480 nm) was recorded and the intensity of the emission increased exponentially with respect to the power density of the 532 nm laser (Figure 6).

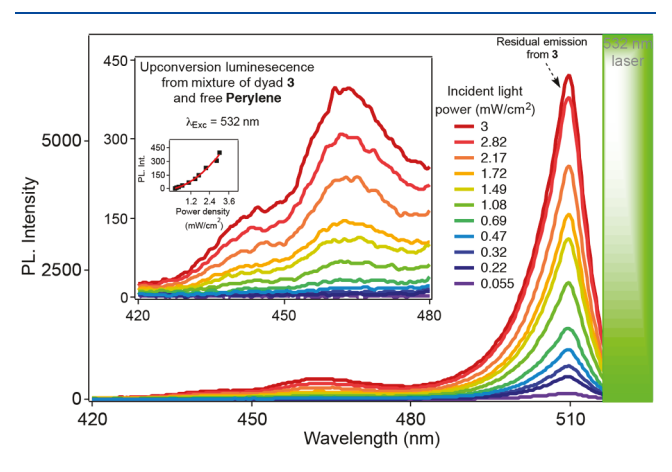


Figure 6. 532 nm light power density dependent upconverted/delayed photoluminescence of free perylene using dyad 3 as light-harvesting triplet sensitizer. The emission spectra were recorded using sample of dyad 3 (O.D. = 0.2 at 532 nm) saturated with recrystallized perylene. Inset: Quadratic response of the upconverted emission intensity at $\lambda_{\rm Em}=465$ nm with respect to the power density of the incident 532 nm laser. See the Experimental Section for additional details/descriptions of the spectrometer setup.

Importantly, this delayed emission in the blue spectral region was not observed with a solution of the dyad alone. It should be noted that the quantum yield of the photon upconversion with a mixture of dyad 3 and perylene is significantly lower than what was previously recorded using free QDN 1 and perylene.²⁷

CONCLUSION

A polyaromatic triplet donor-acceptor dyad 3 was synthesized and fully characterized using absorption and emission spectroscopy techniques as well as time-resolved transient absorption spectroscopy methods. In addition to exhibiting the characteristic absorption and emission from the chromophoric constituents 1 and 2, dyad 3 was also found to produce (CT)* states upon photoexcitation. The CT interaction 1...2 is manifested in the fs-TA of dyad 3 in the 620 to 720 nm spectral region of the fs-TA. This observation correlates with the empirical results from the TD-DFT calculations. Additional photophysical studies revealed that the intradyad 1...2 interaction is dominated by charge transfer dynamics rather than a complete triplet energy transfer. These results are in agreement with the unmatched optoelectronic bandgap of QDN 1 and Per 2, which is required for a Dexter-type ET. However, dyad 3 can still perform intermolecular triplet energy transfer to free perylene resulting in TTA-UC. The present results with dyad 3 add new scores to the library of purely organic donor-acceptor systems and also opens up new avenues for the proper design of chromophoric systems for light harvesting and modulation/transformation.

ASSOCIATED CONTENT

Supporting Information

The Supporting Information is available free of charge at https://pubs.acs.org/doi/10.1021/acs.jpcc.0c01530.

Details of the synthetic procedures for all precursor of dyad 3: ¹H and ¹³C NMR spectra, additional UV-vis absorption spectra, emission spectra, and computational data (PDF)

AUTHOR INFORMATION

Corresponding Author

A. Jean-Luc Ayitou — Department of Chemistry, Illinois Institute of Technology, Chicago, Illinois 60616, United States;
ocid.org/0000-0001-6355-2564; Phone: +1 (312) 567 3454; Email: aayitou@iit.edu

Authors

Young Ju Yun — Department of Chemistry, Illinois Institute of Technology, Chicago, Illinois 60616, United States;
ocid.org/0000-0002-8612-4244

Nareshbabu Kamatham — Department of Chemistry, Illinois Institute of Technology, Chicago, Illinois 60616, United States Manoj K. Manna — Department of Chemistry, Illinois Institute of Technology, Chicago, Illinois 60616, United States

Jingbai Li – Department of Chemistry, Illinois Institute of Technology, Chicago, Illinois 60616, United States

Shuyang Liu – Department of Chemistry, Illinois Institute of Technology, Chicago, Illinois 60616, United States

Gary P. Wiederrecht — Center for Nanoscale Materials, Argonne National Laboratory, Argonne, Illinois 60439, United States

David J. Gosztola — Center for Nanoscale Materials, Argonne National Laboratory, Argonne, Illinois 60439, United States; orcid.org/0000-0003-2674-1379

Benjamin T. Diroll — Center for Nanoscale Materials, Argonne National Laboratory, Argonne, Illinois 60439, United States; orcid.org/0000-0003-3488-0213 Andrey Yu Rogachev — Department of Chemistry, Illinois Institute of Technology, Chicago, Illinois 60616, United States; orcid.org/0000-0001-9855-7824

Complete contact information is available at: https://pubs.acs.org/10.1021/acs.jpcc.0c01530

Notes

The authors declare no competing financial interest.

ACKNOWLEDGMENTS

N.K. is thankful for the generous support as Postdoctoral Fellowship from the Center for Interdisciplinary Scientific Computation (CISC) at Illinois Tech. A.Y.R. thanks the Wanger Institute for Sustainable Energy Research (WISER) for the generous support (WISER Seed Grant). This material is also based upon work supported by the National Science Foundation under a CAREER Grant No. 1753012 Awarded to A.J.A.. Use of the Center for Nanoscale Materials, an Office of the Science user facility, was supported by the U.S. Department of Energy, Office of Science, Office of Basic Energy Science, under Contract No. DE-AC02-06CH11357.

REFERENCES

- (1) Wasielewski, M. R. Self-Assembly Strategies for Integrating Light Harvesting and Charge Separation in Artificial Photosynthetic Systems. *Acc. Chem. Res.* **2009**, *42* (12), 1910.
- (2) Laquai, F.; Park, Y.-S.; Kim, J.-J.; Basché, T. Excitation Energy Transfer in Organic Materials: From Fundamentals to Optoelectronic Devices. *Macromol. Rapid Commun.* **2009**, *30* (14), 1203.
- (3) Kulkarni, A. P.; Kong, X.; Jenekhe, S. A. High-Performance Organic Light-Emitting Diodes Based on Intramolecular Charge-Transfer Emission From Donor—Acceptor Molecules: Significance of Electron- Donor Strength and Molecular Geometry. *Adv. Funct. Mater.* **2006**, *16* (8), 1057.
- (4) Hu, J.-Y.; Yamato, T. Synthesis and Photophysical Properties of Pyrene-Based Light-Emitting Monomers: Highly Blue Fluorescent Multiply-Conjugated-Shaped Architectures. *Organic Light Emitting Diode-Material, Process and Devices*, 2011.
- (5) Xie, F.-M.; Li, H.-Z.; Dai, G.-L.; Li, Y.-Q.; Cheng, T.; Xie, M.; Tang, J.-X.; Zhao, X. Rational Molecular Design of Dibenzo[a,c]-Phenazine-Based Thermally Activated Delayed Fluorescence Emitters for Orange-Red OLEDs with EQE up to 22%. ACS Appl. Mater. Interfaces 2019, 11 (29), 26144.
- (6) Dong, S.-C.; Zhang, L.; Liang, J.; Cui, L.-S.; Li, Q.; Jiang, Z.-Q.; Liao, L.-S. Rational Design of Dibenzothiophene-Based Host Materials for PHOLEDs. J. Phys. Chem. C 2014, 118 (5), 2375.
- (7) Li, L.; Lo, W.-Y.; Cai, Z.; Zhang, N.; Yu, L. Donor—Acceptor Porous Conjugated Polymers for Photocatalytic Hydrogen Production: the Importance of Acceptor Comonomer. *Macromolecules* **2016**, 49 (18), 6903.
- (8) Hayat, A.; Rahman, M. U.; Khan, I.; Khan, J.; Sohail, M.; Yasmeen, H.; Liu, S.-Y.; Qi, K.; Lv, W. Conjugated Electron Donor-Acceptor Hybrid Polymeric Carbon Nitride as a Photocatalyst for CO₂ Reduction. *Molecules* **2019**, 24 (9), 1779.
- (9) Williams, R. M.; Vân Anh, N.; van Stokkum, I. H. M. Triplet Formation by Charge Recombination in Thin Film Blends of Perylene Red and Pyrene: Developing a Target Model for the Photophysics of Organic Photovoltaic Materials. *J. Phys. Chem. B* **2013**, *117* (38), 11239.
- (10) Gong, J.; Sumathy, K.; Qiao, Q.; Zhou, Z. Review on Dye-Sensitized Solar Cells (DSSCs): Advanced Techniques and Research Trends. Renewable Sustainable Energy Rev. 2017, 68, 234.
- (11) Mothika, V. S.; Sutar, P.; Verma, P.; Das, S.; Pati, S. K.; Maji, T. K. Regulating Charge-Transfer in Conjugated Microporous Polymers for Photocatalytic Hydrogen Evolution. *Chem. Eur. J.* **2019**, 25 (15), 3867.

- (12) Wang, J.; Chai, Z.; Liu, S.; Fang, M.; Chang, K.; Han, M.; Hong, L.; Han, H.; Li, Q.; Li, Z. Organic Dyes Based on Tetraaryl-1,4-Dihydropyrrolo-[3,2-b]Pyrroles for Photovoltaic and Photocatalysis Applications with the Suppressed Electron Recombination. *Chem. Eur. J.* **2018**, 24 (68), 18032.
- (13) Ramanan, C.; Kim, C. H.; Marks, T. J.; Wasielewski, M. R. Excitation Energy Transfer Within Covalent Tetrahedral Perylenediimide Tetramers and Their Intermolecular Aggregates. *J. Phys. Chem.* C 2014, 118 (30), 16941.
- (14) Veldman, D.; Chopin, S. M. A.; Meskers, S. C. J.; Groeneveld, M. M.; Williams, R. M.; Janssen, R. A. J. Triplet Formation Involving a Polar Transition State in a Well-Defined Intramolecular Perylenediimide Dimeric Aggregate. J. Phys. Chem. A 2008, 112 (26), 5846.
- (15) Würthner, F. Dipole–Dipole Interaction Driven Self-Assembly of Merocyanine Dyes: From Dimers to Nanoscale Objects and Supramolecular Materials. *Acc. Chem. Res.* **2016**, 49 (5), 868.
- (16) Fernández-Ariza, J.; Krick Calderón, R. M.; Rodríguez-Morgade, M. S.; Guldi, D. M.; Torres, T. Phthalocyanine—Perylenediimide Cart Wheels. *J. Am. Chem. Soc.* **2016**, *138* (39), 12963.
- (17) Luo, C.; Guldi, D. M.; Imahori, H.; Tamaki, K.; Sakata, Y. Sequential Energy and Electron Transfer in an Artificial Reaction Center: Formation of a Long-Lived Charge-Separated State. *J. Am. Chem. Soc.* **2000**, 122 (28), 6535.
- (18) Tuffy, B. Porphyrin Materials for Organic Light Emitting Diodes, 2011.
- (19) Shao, S.; Gobeze, H. B.; Bandi, V.; Funk, C.; Heine, B.; Duffy, M. J.; Nesterov, V.; Karr, P. A.; D'Souza, F. Triplet BODIPY and AzaBODIPY Derived Donor-Acceptor Dyads: Competitive Electron Transfer Versus Intersystem Crossing Upon Photoexcitation. *ChemPhotoChem.* 2020, 4, 68.
- (20) Chen, Q.; Liu, Y.; Guo, X.; Peng, J.; Garakyaraghi, S.; Papa, C. M.; Castellano, F. N.; Zhao, D.; Ma, Y. Energy Transfer Dynamics in Triplet—Triplet Annihilation Upconversion Using a Bichromophoric Heavy-Atom-Free Sensitizer. *J. Phys. Chem. A* **2018**, *122* (33), *6673*.
- (21) Zaumseil, J.; Sirringhaus, H. Electron and Ambipolar Transport in Organic Field-Effect Transistors. *Chem. Rev.* **2007**, *107* (4), 1296. (22) Li, C.; Liu, M.; Pschirer, N. G.; Baumgarten, M.; Müllen, K. Polyphenylene-Based Materials for Organic Photovoltaics. *Chem. Rev.* **2010**, *110* (11), 6817.
- (23) Chen, W.; Yang, X.; Long, G.; Wan, X.; Chen, Y.; Zhang, Q. A Perylene Diimide (PDI)-Based Small Molecule with Tetrahedral Configuration as a Non-Fullerene Acceptor for Organic Solar Cells. *J. Mater. Chem. C* **2015**, *3* (18), 4698.
- (24) Huang, G.-J.; Harris, M. A.; Krzyaniak, M. D.; Margulies, E. A.; Dyar, S. M.; Lindquist, R. J.; Wu, Y.; Roznyatovskiy, V. V.; Wu, Y.-L.; Young, R. M.; Wasielewski, M. R. Photoinduced Charge and Energy Transfer Within Meta- and Para-Linked Chlorophyll a-Perylene-3,4:9,10-Bis(Dicarboximide) Donor—Acceptor Dyads. *J. Phys. Chem. B* **2016**, *120* (4), 756.
- (25) Yoo, H.; Bahng, H. W.; Wasielewski, M. R.; Kim, D. Polymer Matrix Dependence of Conformational Dynamics Within a Π-Stacked Perylenediimide Dimer and Trimer Revealed by Single Molecule Fluorescence Spectroscopy. *Phys. Chem. Chem. Phys.* **2012**, *14* (6), 2001.
- (26) Margulies, E. A.; Miller, C. E.; Wu, Y.; Ma, L.; Schatz, G. C.; Young, R. M.; Wasielewski, M. R. Enabling Singlet Fission by Controlling Intramolecular Charge Transfer in π , π –Stacked Covalent Terrylenediimide Dimers. *Nat. Chem.* **2016**, 8 (12), 1120.
- (27) Shokri, S.; Wiederrecht, G. P.; Gosztola, D. J.; Ayitou, A. J.-L. Photon Upconversion Using Baird-Type (Anti)Aromatic Quinoidal Naphthalene Derivative as a Sensitizer. *J. Phys. Chem. C* **2017**, *121* (42), 23377.
- (28) Manna, M. K.; Shokri, S.; Wiederrecht, G. P.; Gosztola, D. J.; Ayitou, A. J.-L. New Perspectives for Triplet—Triplet Annihilation Based Photon Upconversion Using All-Organic Energy Donor & Acceptor Chromophores. *Chem. Commun.* **2018**, 54 (46), 5809.

- (29) Grimme, S.; Brandenburg, J. G.; Bannwarth, C.; Hansen, A. Consistent Structures and Interactions by Density Functional Theory with Small Atomic Orbital Basis Sets. *J. Chem. Phys.* **2015**, *143* (5), 054107.
- (30) Kruse, H.; Grimme, S. A Geometrical Correction for the Interand Intra-Molecular Basis Set Superposition Error in Hartree-Fock and Density Functional Theory Calculations for Large Systems. *J. Chem. Phys.* **2012**, *136* (15), 154101.
- (31) Grimme, S.; Ehrlich, S.; Goerigk, L. Effect of the Damping Function in Dispersion Corrected Density Functional Theory. *J. Comput. Chem.* **2011**, 32 (7), 1456.
- (32) Grimme, S.; Antony, J.; Ehrlich, S.; Krieg, H. A Consistent and Accurate Ab Initio Parametrization of Density Functional Dispersion Correction (DFT-D) for the 94 Elements H-Pu. *J. Chem. Phys.* **2010**, 132 (15), 154104.
- (33) Kendall, R. A.; Früchtl, H. A. The Impact of the Resolution of the Identity Approximate Integral Method on Modern Ab Initio Algorithm Development. *Theor. Chem. Acc.* **1997**, *97* (1), 158.
- (34) Weigend, F. Accurate Coulomb-Fitting Basis Sets for H to Rn. *Phys. Chem. Chem. Phys.* **2006**, 8 (9), 1057.
- (35) Neese, F. The ORCA Program System. Wiley Interdiscip. Rev.: Comput. Mol. Sci. 2012, 2, 73–78.
- (36) Shokri, S.; Li, J.; Manna, M. K.; Wiederrecht, G. P.; Gosztola, D. J.; Ugrinov, A.; Jockusch, S.; Rogachev, A. Y.; Ayitou, A. J.-L. A Naphtho- p-Quinodimethane Exhibiting Baird's (Anti)Aromaticity, Broken Symmetry, and Attractive Photoluminescence. J. Org. Chem. 2017, 82 (19), 10167.
- (37) Shoer, L. E.; Eaton, S. W.; Margulies, E. A.; Wasielewski, M. R. Photoinduced Electron Transfer in 2,5,8,11-Tetrakis-Donor-Substituted Perylene-3,4:9,10-Bis(Dicarboximides). *J. Phys. Chem. B* **2015**, 119 (24), 7635.
- (38) Margulies, E. A.; Shoer, L. E.; Eaton, S. W.; Wasielewski, M. R. Excimer Formation in Cofacial and Slip-Stacked Perylene-3,4:9,10-Bis(Dicarboximide) Dimers on a Redox-Inactive Triptycene Scaffold. *Phys. Chem. Phys.* **2014**, *16* (43), 23735.
- (39) Perdew, J.; Burke, K.; Ernzerhof, M. Generalized Gradient Approximation Made Simple. *Phys. Rev. Lett.* **1996**, 77 (18), 3865.
- (40) Perdew, J. P.; Burke, K.; Ernzerhof, M. Generalized Gradient Approximation Made Simple [Phys. Rev. Lett. 77, 3865 (1996)]. Phys. Rev. Lett. 1997, 78 (7), 1396.